Check for updates

View Article Online
View Journal

Dalton Transactions

An international journal of inorganic chemistry

Accepted Manuscript

This article can be cited before page numbers have been issued, to do this please use: S. Li, G. Xu, Y. Zhu, J. Zhao and S. Gou, *Dalton Trans.*, 2020, DOI: 10.1039/D0DT01040E.

This is an Accepted Manuscript, which has been through the Royal Society of Chemistry peer review process and has been accepted for publication.

Accepted Manuscripts are published online shortly after acceptance, before technical editing, formatting and proof reading. Using this free service, authors can make their results available to the community, in citable form, before we publish the edited article. We will replace this Accepted Manuscript with the edited and formatted Advance Article as soon as it is available.

You can find more information about Accepted Manuscripts in the Information for Authors.

Please note that technical editing may introduce minor changes to the text and/or graphics, which may alter content. The journal's standard Terms & Conditions and the Ethical guidelines still apply. In no event shall the Royal Society of Chemistry be held responsible for any errors or omissions in this Accepted Manuscript or any consequences arising from the use of any information it contains.

ROYAL SOCIETY OF CHEMISTRY

rsc.li/dalton

View Article Online
DOI: 10.1039/D0DT01040E

ARTICLE

Bifunctional Ruthenium(II) Polypyridyl Complexes of Curcumin as Potential Anticancer Agents

Received 00th January 20xx,
Accepted 00th January 20xx

DOI: 10.1039/x0xx00000x

Shuang Li,† [a] Gang Xu,† [a] Yuhua Zhu,[b] Jian Zhao,*[a] Shaohua Gou*[a]

Ru(II)-polypyridyl complexes have been widely studied and well established for their antitumor properties. Modifications of the coordination environment around the Ru atom through proper choice of the ligand can lead to different modes of action and result in greatly improved anticancer efficacy. Herein, two Ru(II)-polypyridyl complexes of curcumin were synthesized and characterized as potential anticancer agents. In vitro tests indicated that complexes **1** and **2** displayed excellent antiproliferative activity against the tested cancer cell lines, especially complex **2**, which exhibited superior cytotoxicity compared to curcumin and cisplatin. Further biological evaluations demonstrated that complexes **1** and **2** can cause cell apoptosis via DNA interaction and MEK/ERK signaling pathway, which is the first example of a Ru(II)-polypyridyl complex to inhibit MEK/ERK signaling pathway as well as DNA intercalation. Overall, this work suggests that coordination with bioactive agents may endow Ru(II)-polypyridyl complexes with improved pharmaceutical properties and synergistic effects for cancer therapy.

INTRODUCTION

Platinum-based drugs, as outstanding representatives of chemotherapeutic drugs, have been successfully applied in the clinical treatment of various solid tumors.[1] However, their clinical applications are obstructed on account of severe side effects and insurmountable drug resistance.[2] Under such circumstances, many other metal complexes, especially Ru-based complexes, have been designed and explored as alternative agents for cancer therapy. For example, three notable Ru-based complexes (NAMI-A, NKP-1339 and TLD1433) have entered clinical trials, which has spurred attempts to develop novel Ru-based agents with different modes of action for cancer therapy.[3] Over the last two decades, Ru(II)-polypyridyl complexes have been showing great potential in biomedical applications due to their unique biological and physiochemical features,[4] For example, Ru(II)-polypyridyl complexes have the ability to bind with different biological targets upon the modification of the ligands.[5] As a result, Ru(II)-polypyridyl complexes have been extensively developed and evaluated for their antitumor activities and some of which have shown great potential as anticancer candidates.[6]

Curcumin, a β-diketone polyphenol originated from the rhizome of the herbaceous turmeric (*Curcuma longa*), is a promising candidate for cancer therapy. Although the underlying anticancer mechanisms of curcumin has not been thoroughly explored, its tumor selectivity and low side effects has sparked a large number of clinical trials.[7] However, the clinical application of curcumin is still stagnant due to its poor water solubility, little tissue accumulation and instability under physiological conditions.[8] Thus, improving the hydrolytic stability of curcumin is crucial for promoting its clinical treatment. Benefiting from the β-diketone structure of curcumin, it can form thermodynamically stable compounds with many metal complexes cations, enabling them to reach biological targets without decomposition,[9] and some of the complexes showed potent anticancer efficacy both in vitro and in vivo.[10] Remarkably, arene-Ru(II) complexes of curcumin have been widely studied as potential anticancer agents. For example, the complex [(p-cymene)Ru(cur)Cl] has been developed and reported by Caruso and co-workers, which exhibited superior cytotoxicity in the HCT116 cells.[11] Subsequently, the same group found that the anticancer activity of arene-ruthenium(II) curcuminoid complexes may be correlated with increase of curcuminoid lipophilicity.[12] Besides, Dyson and co-workers have developed several RAPTA-type Ru(II)-(arene)-curcumin complexes with good aqueous solubility and excellent anticancer efficacy.[13]

It is worth noting that modifications of the coordination environments of Ru(II)-polypyridyl complexes through proper choice of the ligand can lead to different modes of action and greatly improved anticancer efficacy.[14] To date, limited efforts have been made in designing Ru(II)-polypyridyl complexes with curcumin ligand for anticancer study. Based on the studies above, we intended to utilize $[Ru(bpy)_3]Cl_2$ as a model complex and take the place of its one bipyridine by curcumin to get

[a] Jiangsu Province Hi-Tech Key Laboratory for Biomedical Research and Pharmaceutical Research Center, School of Chemistry and Chemical Engineering, Southeast University, Nanjing 211189, P. R. China.
[b] State Key Laboratory of Analytical Chemistry for Life Science, Nanjing University, Nanjing 210093, P. R. China.
† These authors contributed equally to this work.
Electronic Supplementary Information (ESI) available: See DOI: 10.1039/x0xx00000x

Published on 18 June 2020. Downloaded by East Carolina University on 6/18/2020 11:39:13 AM.

Dalton Transactions Accepted Manuscript

View Article Online
DOI: 10.1039/D0DT01040F

complex **1** (Figure 1). Notably, complex **1** displayed potent antimicrobial activity both in vitro and in vivo.[15] It has been reported that dppz-containing Ru(II) complexes (dppz = dipyrido[3,2-a:2', 3'-c]phenazine) can intercalate between DNA base pairs and serve as DNA molecular light switches.[16] The dppn (benzo-[i]dipyrido[3,2-a:2',3'-c]phenazine) is a derivative of dppz, which may have the potential to intercalate into DNA due to its excellent planar conjugated structure.[17] Thus, to further improve the DNA binding ability as well as in vitro anticancer activity of complex **1**, another bipyridine in complex **1** was replaced with dppn to obtain complex **2**. These two Ru(II)-polypyridyl complexes with curcumin as ligand were designed as potential anticancer agents, with the goal of increasing the hydrolytic stability of curcumin and improving the pharmacological activity of the Ru(II)-polypyridyl complexes. Herein, two ruthenium(II) polypyridyl complexes of curcumin were synthesized, and their biological activities as well as potential anticancer mechanisms were explored.

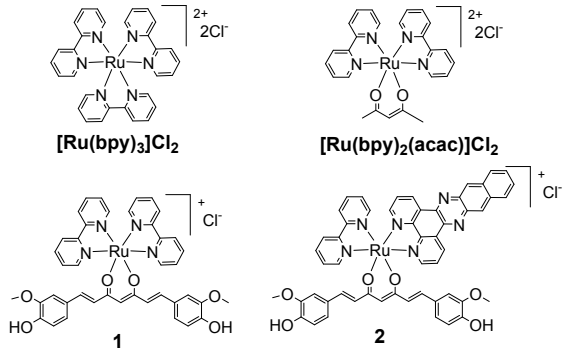

Fig. 1 Ru(II)-polypyridyl complexes studied in this work.

Results and discussion

Synthesis and characterization

Scheme 1 Chemical Structures and Synthetic Procedures of Complex **2**.

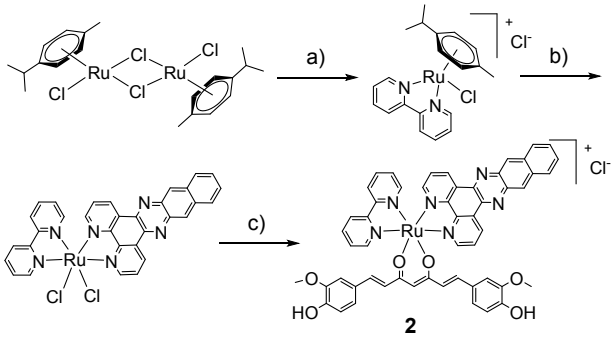

Reagents and conditions: a) MeOH, bpy, reflux, 12 h; b) dppn, LiCl, DMF, reflux, 4 h; c) curcumin, LiCl, EtOH/H_2O (3:1), reflux, 12 h.

Complex **1** was prepared according to previous literature,[15] and complex **2** was synthesized by following the steps outlined in Scheme 1. The composition and purity of complexes **1** and **2** were determined by ^{1}H and ^{13}C NMR spectra, ESI-MS spectroscopy along with elemental analysis (Fig. S1-S6). $Ru(bpy)_2(acac)]Cl_2$ was synthesized as control, which was characterized by ^{1}H NMR spectra (Figures S7). The absorption and emission spectra of complexes **1** and **2** were studied (Fig. 2). Notably, the photoluminescence intensity of the complexes **1** and **2** was extremely low in aerated solution. Therefore, the emission spectra of complexes **1** and **2** were further measured in deaerated methanol solution (Fig. 2b). The emission spectra of complexes **1** and **2** are located at around 620 nm, which are red-shifted compared to the emission of curcumin located at around 550 nm. Overall, the emission spectrum may be attributed to phosphorescence from ^{3}MLCT (metal-to-ligand charge transfer) transitions.

Stability and lipophilicity

The stability of **1** and **2** was evaluated by observing the electronic spectral changes at different times in hepes buffer (pH = 7.2). As shown in Figure S7, minor changes of the absorption spectra were observed for complexes **1** and **2** within 4 h. In contrast, the absorption bands of curcumin decreased dramatically fast, indicating the degradation of curcumin under the tested conditions. This study indicated that coordination of curcumin to Ru(II)-polypyridyl moiety can prevent the hydrolysis of curcumin under physiological conditions.

The lipophilicity of the compounds is highly associated with cellular uptake.[14(c)] Therefore, the log *P* (the octanol-water partition coefficient) values of complexes **1**-**2** and $[Ru(bpy)_2(acac)]Cl_2$ were measured using the shake-flask method. As revealed in Table 1, The log *P* values of **1** and **2** were 0.75 and 1.06, respectively, both of which were higher than those of $[Ru(bpy)_2(acac)]Cl_2$ (-1.2) and $[Ru(bpy)_3]Cl_2$ (-0.41), implying that complexes **1-2** have higher lipophilicity than $[Ru(bpy)_2(acac)]Cl_2$ and $[Ru(bpy)_3]Cl_2$.

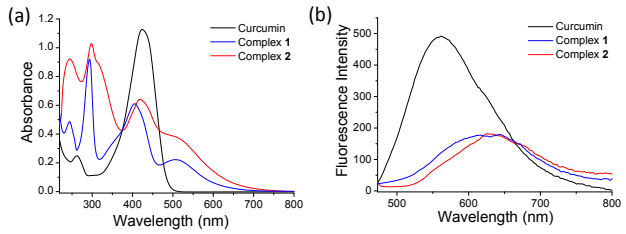

Fig. 2 UV-vis absorbance (a) and emission spectra (b) of curcumin and complexes **1** and **2** in MeOH (20 μM). Emission spectra of **1** (λ_{ex} = 420 nm) and **2** (λ_{ex} = 450 nm) were measured in deaerated MeOH.

Electrostatic potential maps

The electrostatic potential surfaces (ESP) of **1** and **2** were obtained by density functional theory (DFT) calculations.[18] As shown in Fig. 3, the relatively green-colored region at the curcumin moiety in complexes **1** and **2** defined a region of high electron density. The corresponding blue area at bipyridine moiety depicts a diminished electronic density. In general, a similar profile was observed for complexes **1** and **2**, except that electron density at dppn moiety in complex **2** is higher than bipyridine moiety in complex **1**.

Published on 18 June 2020. Downloaded by East Carolina University on 6/18/2020 11:39:13 AM.

Dalton Transactions Accepted Manuscript

This journal is © The Royal Society of Chemistry 20xx

View Article Online
DOI: 10.1039/D0DT01405

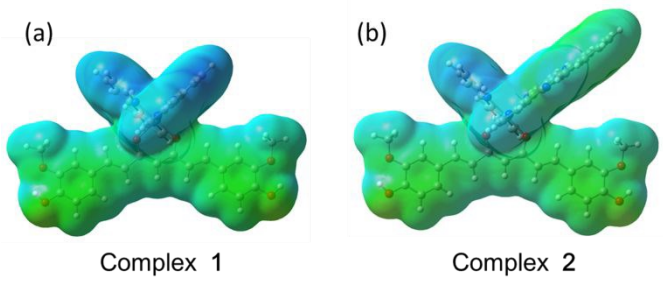

Fig. 3 Electrostatic potential surfaces of complexes **1** (a) and **2** (b). ESP maps (from -0.10 au in green, to +0.15 au in blue) drawn onto an electron density isosurface (0.004 au) for the same compounds.

In vitro cytotoxicity study

The antiproliferative properties of complexes **1** and **2** were evaluated against A549 (human non-small-cell lung cancer), MCF-7 (human breast adenocarcinoma) and SGC7901 (human gastric cancer) cell lines together with curcumin, cisplatin, $[Ru(bpy)_3]Cl_2$ and $[Ru(bpy)_2(acac)]Cl_2$ for comparison by using the MTT assay. As shown in Table 1 and Figure S9, both complexes **1** and **2** exhibited considerable cytotoxicity against the tested cancer cell lines with IC_{50} values ranging from 2.1 to 5.8 μM. Comparing $[Ru(bpy)_2(acac)]Cl_2$ and complex **1**, the IC_{50} values of $[Ru(bpy)_2(acac)]Cl_2$ against A549 (8.6 μM), MCF-7 (11.7 μM), and SGC7901 (10.3 μM) cells are much higher than those of complex **1** (3.8, 5.2 and 5.8 μM, respectively), thus indicating that replacing acetylacetone in $[Ru(bpy)_2(acac)]Cl_2$ with curcumin can greatly improve the cytotoxicity of complex **1**. Importantly, complex **2** showed much superior activity to those of reference compounds against the tested cancer cell lines, which were > 17.0-, > 5.7- and > 4.8-fold as potent as $[Ru(bpy)_3]Cl_2$, curcumin and cisplatin, respectively, demonstrating that introduction of curcumin to the Ru(II)-polypyridyl moieties is an effective way to improve the cytotoxic activity of the Ru(II)-polypyridyl complexes.

Table 1 Log *P* values and cytotoxicity data for complexes **1**-**2**, curcumin, Cisplatin, $[Ru(bpy)_3]Cl_2$ and $[Ru(bpy)_2(acac)]Cl_2$

Compound	IC_{50} values (μM) [a]			log*P*
	A549 [b]	MCF-7 [c]	SGC7901 [d]	
1	3.8 ± 0.2	5.2 ± 0.4	5.8 ± 0.4	0.75
2	2.1 ± 0.2	2.3 ± 0.1	2.7 ± 0.2	1.06
Curcumin	13.1 ± 1.1	13.0 ± 0.9	15.4 ± 1.0	ND[e]
Cisplatin	13.8 ± 0.7	11.4 ± 0.3	13.0 ± 0.9	-2.03[f]
$[Ru(bpy)_3]Cl_2$	47.5 ± 1.9	39.2 ± 2.8	> 50.0	-0.41[g]
$[Ru(bpy)_2(acac)]Cl_2$	8.6 ± 0.3	11.7 ± 0.8	10.3 ± 0.5	-1.2

[a] The IC_{50} values were determined after 72 h of drug exposure; [b] human non-small-cell lung cancer; [c] human breast adenocarcinoma cell line; [d] human gastric cancer cell line; [e]Not determined; [f]Cited from ref 19; [g]Cited from ref 20.

To further visually assess the cytotoxicity induced by complexes **1** and **2** against cancer cells, calcein AM and propidium iodide (PI) co-staining assay was performed to dye the living and dead cells. As shown in Fig. 4, A549 cells maintained high viability for the control group. However, cells treated with complexes **1** and **2** were effectively killed as revealed by the intense red fluorescence, demonstrating the considerable antitumor potency of **1** and **2**. More effective anticancer activity of complex **2** was observed from a lower proportion of living cells as compared with **1**, which was in correspondence with the results of IC_{50} values.

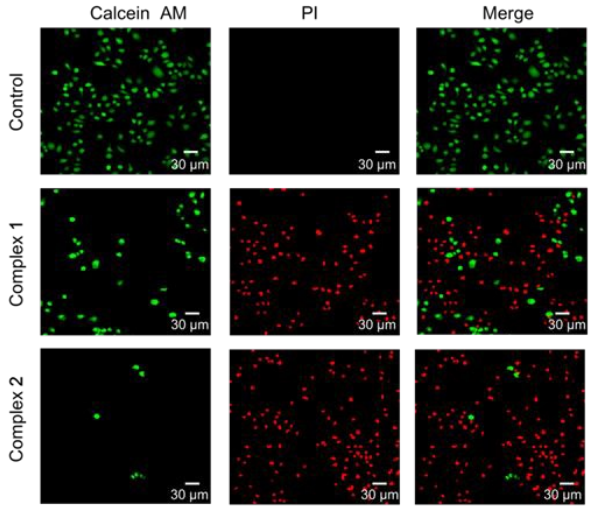

Fig. 4 Fluorescence images of A549 cells co-stained with calcein AM and propidium iodide (PI) after 24 h of treatment with complexes **1** and **2** at concentration of 10 μM (size bar = 30 μm).

DNA interaction

DNA is the main target for Ru(II)-polypyridyl complexes, which generally interact with DNA through electrostatic interaction, intercalation and/or groove binding.[5(b), 5(c)] In order to investigate the interaction pattern between **1**, **2** and DNA, competitive binding experiments were executed by monitoring the emission intensity of DNA-bound ethidium bromide (EB) upon the addition of **1** and **2**. It was reported that the fluorescence intensity can be reduced by DNA groove binders or intercalators. Nevertheless, the reduction induced by groove binders is moderate, while intercalators can reduce the intensity significantly as a consequence of the replacement of EB.[21] As exhibited in Figure 5, the emission intensity of CT-DNA-EB system (λ_{ex} = 537 nm and λ_{em} = 597 nm) gradually decreased with increasing the concentration of two complexes, demonstrating complexes **1**-**2** can interact with DNA through groove binding or intercalation. Furthermore, it was apparent that the decrease of fluorescence intensity of CT-DNA-EB complex caused by complex **2** was more severe than that of complex **1**. To futher illustrate the DNA binding affinity of **1**-**2**, the value of the apparent DNA binding constant (K_{app}) were calculated using the following equation.

$$K_{EB}\,[EB]=K_{app}\,[complex]$$

Published on 18 June 2020. Downloaded by East Carolina University on 6/18/2020 11:39:13 AM.

Dalton Transactions Accepted Manuscript

View Article Online
DOI: 10.1039/D0DT01040F

Where K_{EB} (4.94 × 10^5 M^{-1}) is the average DNA binding constant of EthBr,[22] [EB] is the concentration of EB (25 μM), [complex] is the concentration of the complex at 50% fluorescence intensity from the plots of the relative intensities I/I0 against the concentrations of complexes **1**-**2**. The Kapp values for **1** and **2** are 4.79 × 10^5 M^{-1} and 1.14 × 10^6 M^{-1} respectively, implying that complex **2** with dppn ligand showed higher DNA-binding ability relative to complex **1** with bipyridine ligand.

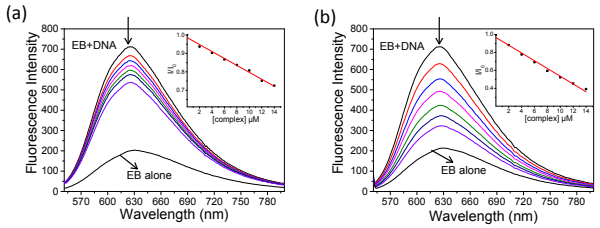

Fig. 5 Fluorescence emission spectra of CT-DNA-EtBr quenched by increasing the concentrations of complexes **1** (a) and **2** (b). [CT-DNA] = 50 μM; [EB] = 25 μM; [complex] = 0-14 μM.

Molecular docking studies of complexes **1** and **2** with a DNA duplex structure (PDB ID: 4jd8) were carried out using Autodock 4.2 package.[23] As presented in Fig. 6, the predicted optimal binding mode of complex **1** and DNA showed that the curcumin skeleton of complex **1** fit into the groove of the DNA in a parallel manner with respect to the DNA backbone. However, a very different mode was observed for complex **2**, which showed that the dppn ligand intercalated between DNA base pairs like dppz-containing Ru(II) complexes. The binding energies of complexes **1** and **2** with DNA were -5.77 and -11.05 kcal/mol, respectively, indicating that complex **2** with dppn ligand exhibited higher DNA-binding ability, which is in accordance with the competitive binding experiments. Taken together, DNA binding studies imply that complex **1** may interact with DNA through groove binding, while complex **2** is proposed to interact with DNA via intercalation.

Celllular uptake

Both cellular uptake and subcellular location are crucial factors impacting the biological activities of compounds.[4] Given weak luminescence of complexes **1**-**2**, inductively coupled plasma mass spectrometry (ICP-MS) was used to measure cellular uptake efficacy of **1**, **2** and $[Ru(bpy)_2(acac)]Cl_2$ in A549 cells. As revealed by Figure S10, the amount of cellular uptake for complex **2** (65.4 pmol/10^6 cells) was approximately 1.2-time larger than that of **1** (53.5 pmol/10^6 cells), which may be attributed to the higher lipophilicity of **2**. Moreover, the accumulation of both complexes **1** and **2** was higher than that of $[Ru(bpy)_2(acac)]Cl_2$ (41.9 pmol/10^6 cells). Notably, about 56.9% of Ru content of complex **2** was located in nucleus, which was much higher than those of complex **1** (30.1%) and $[Ru(bpy)_2(acac)]Cl_2$ (29.6%). Overall, the increased cellular uptake and nuclear distribution of complex **2** may be responsible for its high cytotoxicity.

Western Blot Study

It was reported that curcumin plays an important role in cell proliferation, differentiation, and apoptosis through the extracellular signal-regulated kinase (ERK) signaling pathway.[24] To further discover the modes of action of the resulting Ru(II) complexes, western blot was performed to investigate the expression of p-ERK1/2 and p-MEK1/2 in Ru(II)-treated A549 cells, since activation of MEK/ERK pathway is mediated through their phosphorylation.[25] As shown in Fig. 7, the expression of p-ERK1/2 was decreased after treatment with **1** and **2**, reflecting the potent efficacy of the Ru(II) complexes in inhibiting enzymatic activity of MEK1 kinase. Moreover, the expression of p-ERK1/2 after treatment with complex **2** was relatively lower than that of complex **1** at concentration of 10 μM (Fig. 7b), demonstrating the stronger inhibitory effect of complex **2**. Besides, it is noted that the phosphorylation of MEK1 was also inhibited by complexes **1** and **2**, indicating that these complexes could also block the phosphorylation of MEK1 by upstream kinase.[26] Taken together, this study confirmed that the Ru(II)-polypyridyl-curcuminato complexes can inhibit the MEK/ERK signaling pathway.

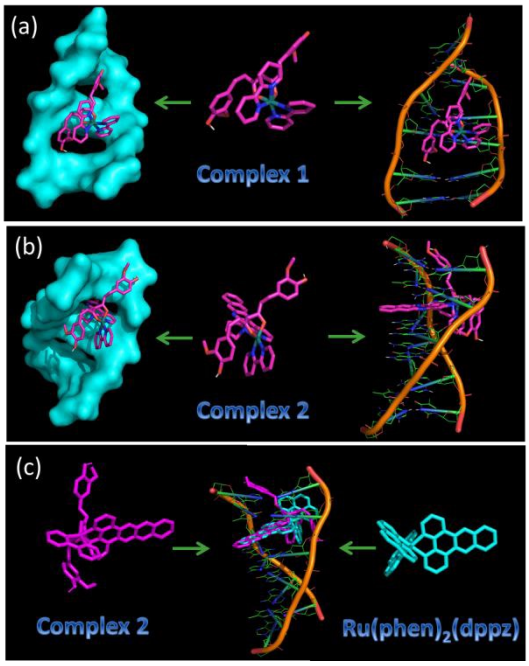

Fig. 6 Molecular docked modes of complexes **1** (a) and **2** (b) with DNA duplex (PDB ID: 4jd8);(c)Docked complex **2** (magenta) superimposed over co-crystallized $[Ru(phen)_2(dppz)]^{2+}$ (cyan).

Cell Cycle Distribution

The effects of complexes **1** and **2** on cell cycle distribution of A549 cells were determined by flow cytometry with propidium iodide (PI) staining. As shown in Fig. 8, complexes **1** and **2** can block the cell cycle at the G0/G1 phase in A549 cells compared to the untreated group (control), which is different from the most of the anticancer agents (eg. cisplatin) that block the cell cycle in the S or G2/M phases, implying the different modes of action of the resulting Ru(II) complexes.[27] Besides, the percentages of cells arrested at the G0/G1 phase by complex **2**

Published on 18 June 2020. Downloaded by East Carolina University on 6/18/2020 11:39:13 AM.

Dalton Transactions Accepted Manuscript

This journal is © The Royal Society of Chemistry 20xx

View Article Online
DOI: 10.1039/D0DT01040E

were higher than those of complex **1** at concentrations of 1 and 5 μM, respectively, demonstrating that treatment with complex **2** affected the G0/G1 populations more than treatment with complex **1**.

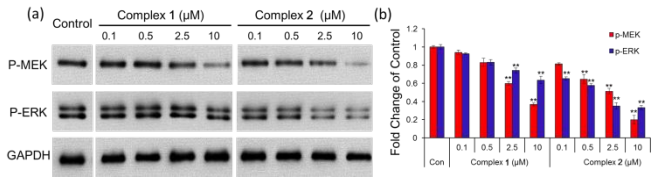

Fig. 7 (a) The expression of p-MEK and p-ERK proteins in A549 cells was analyzed by western blot after being treated with complexes **1** and **2** for 24 h. The data represents three parallel experiments with similar results. (b) The relative expression content of p-MEK and p-ERK proteins was measured through densitometric analysis and normalized with GAPDH. The data was representative of the density of protein band/density of GAPDH band.

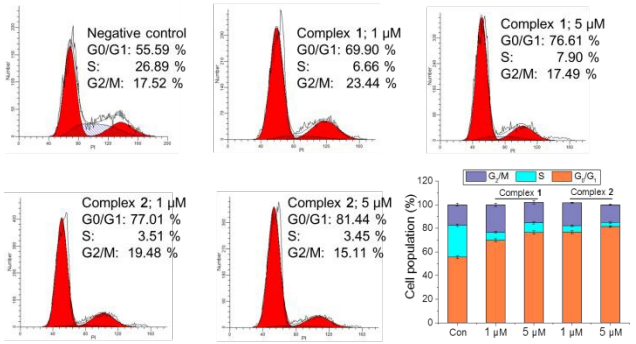

Fig. 8 Cell cycle distribution of A549 cancer cells after being incubated with complexes **1** and **2** at concentrations of 1 μM and 5 μM for 24 h. Data are quoted as mean ± SD of three replicates.

Apoptosis studies

Apoptosis is a means of programmed cell death in multicellular organisms, which generally confers advantages during an organism's life cycle. The potential of complexes **1** and **2** to induce cell death in A549 cells was determined by Annexin V/PI double-labeling assay. As shown in Fig. 9, treatment with **1** and **2** increased the apoptotic populations (early and late apoptotic cells) of A549 cells compared with untreated cells (control). Moreover, the apoptotic rates of the A549 cells were increased with increasing concentrations of complexes **1**-**2**, suggesting that the resulting Ru(II) complexes could induce cancer cell death in a concentration-dependent manner. Overall, this study indicated that complexes **1** and **2** can induce cancer cell death through an apoptotic pathway. Moreover, Hoechst 33358 staining assay was conducted to confirm the cell apoptosis induced by **1** and **2**. As shown in Fig. S9, A549 cells treated with complexes **1** and **2** exhibited cytoplasm shrinkage and fragmentation, accompanied by intensely bright blue fluorescence in nucleus, whereas the control group showed negligible fluorescence intensity, implying that **1** and **2** could induce cancer cell death through an apoptotic pathway.

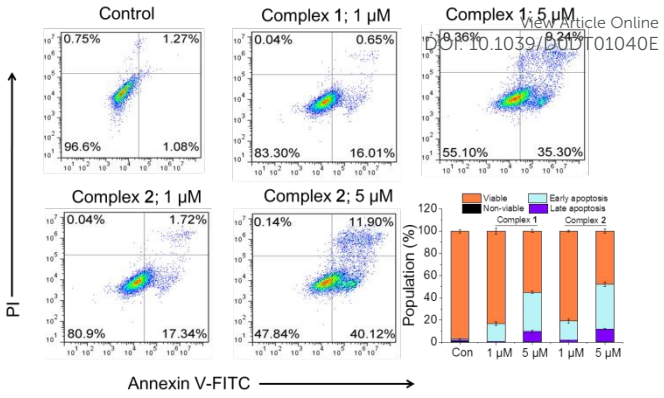

Fig. 9 Apoptosis analysis of A549 cells determined by flow cytometry after treatment with complees **1** and **2** for 24 h. Data are expressed as the mean (± SD) for three independent experiments.

Experimental Section

Materials and Measurements

All reagents are analytically pure and used without additional purification. *cis*-$[Ru(bpy)_2]Cl_2$ and *cis*-$[Ru(bpy)(dppn)]Cl_2$ are synthesized according to previously published literature.[28] Cancer cell lines were obtained from Jiangsu KeyGEN BioTECH company (China), and pBR322 plasmid DNA was purchased from Thermofisher, China. ^1H and ^{13}C NMR spectra were performed on a Bruker Avance III-HD 600 MHz spectrometer. Mass spectroscopy was measured on an Agilent 6224 ESI/TOF MS instrument, and elemental analysis of C, H, and N was performed on a Vario MICRO CHNOS elemental analyzer (Elemental). UV-vis spectra were measured on Shimadzu UV2600 instrument. DNA competitive binding experiments were carried out using a SHIMADZU RF-600 fluorometer. Cell cycle distribution and apoptosis experiments were conducted using flow cytometry (FAC Scan, Becton Dickenson). The cell accumulation of the complexes was conducted on a PerkinElmer NexION® 1000G ICP Mass spectrometer.

General Synthetic Procedure and Characterization of Complexes 1 and 2

cis-$[Ru(bpy)_2Cl_2]$ or *cis*-$[Ru(bpy)(dppn)Cl_2]$ (0.5 mmol), curcumin (368.4 mg, 1.0 mmol) and LiCl (42.0 mg, 1.0 mmol) was adequately mixed in EtOH/H_2O (3:1) and stirred at refluxing temperature for 12 h. A black hybrid solution was obtained, and the solvent was evaporated under vacuum. The final product was purified by using dichloromethane/methanol (50:1, v/v) through preparative column chromatography (basic Al_2O_3).

Complex 1. Yield: 52.0%. Black-brown powder. Anal. Calcd (%) for $C_{41}H_{35}ClN_4O_6Ru$: C 60.33, H 4.32, N 6.86, Found: C 60.18, H 4.37, N 6.97; ESI-MS: $[M - Cl]^+$ = 781.1587; ^1H NMR (600 MHz, DMSO-d_6) δ 3.75 (s, 6H), 5.96 (s, 1H), 6.58-6.61 (d, 2H, J = 15.8 Hz), 6.79-6.81 (d, 2H, J = 8.2 Hz), 6.88-6.90 (m, 2H), 6.95-6.97 (d, 2H, J = 15.7 Hz), 7.11-7.12 (m, 2H), 7.29-7.32 (t, 2H, J = 6.6 Hz), 7.76-7.80 (m, 4H), 7.91-7.93 (t, 2H, J = 7.6 Hz), 8.16-8.19 (t, 2H, J = 7.6 Hz), 8.64-8.65 (d, 2H, J = 5.3 Hz), 8.74-8.76 (d, 2H, J

Published on 18 June 2020. Downloaded by East Carolina University on 6/18/2020 11:39:13 AM.

Dalton Transactions Accepted Manuscript

View Article Online
DOI: 10.1039/D0DT01040B

Published on 18 June 2020. Downloaded by East Carolina University on 6/18/2020 11:39:13 AM.

= 8.0 Hz), 8.85-8.86 (d, 2H, *J* = 8.1 Hz); ^{13}C NMR (150 MHz, DMSO-d_6) δ 56.02, 101.87, 110.68, 116.08, 122.42, 123.97, 124.02, 126.26, 126.39, 126.93, 127.31, 135.44, 136.47, 137.04, 148.39, 148.77, 149.81, 153.23, 157.88, 159.24, 178.20 ppm.

Complex 2. Yield: 40.5%. Black-brown powder. Anal. Calcd (%) for $C_{53}H_{39}ClN_6O_6Ru$: C 64.14, H 3.96, N 8.47. Found: C 63.98, H 4.13, N 8.69; ESI-MS: m/z $[M - Cl]^+$ = 957.2062; ^{1}H NMR (600 MHz, DMSO-d_6) δ 3.54 (s, 3H), 3.79 (s, 3H), 6.09 (s, 1H), 6.60-6.61 (d, 1H, *J* = 8.3 Hz), 6.69-6.71 (d, 2H, *J* = 15.9 Hz), 6.78-6.82 (m, 2H), 6.94-6.95 (m, 1H), 6.99 (m, 1H), 7.06-7.09 (d, 1H, *J* = 15.8 Hz), 7.15-7.17 (m, 2H), 7.21-7.23 (t, 1H, *J* = 6.6 Hz), 7.63 (m, 2H), 7.71-7.72 (m, 1H), 7.83-7.84 (d, 1H, *J* = 5.6 Hz), 7.88-7.93 (m, 2H), 8.09-8.10 (m, 1H), 8.23-8.29 (m, 4H), 8.75-8.77 (d, 1H, *J* = 8.2 Hz), 8.84-8.90 (m, 3H), 8.96 (m, 1H), 9.03-9.04 (d, 2H, *J* = 5.2 Hz), 9.26 (m, 1H), 9.43 (s, 1H), 9.57 (s, 1H); ^{13}C NMR (150 MHz, DMSO-d_6) δ 55.70, 56.10, 102.66, 110.86, 116.06, 116.19, 122.56, 126.15, 126.35, 127.29, 127.36, 127.76, 129.63, 137.45, 140.55, 148.19, 148.47, 148.71, 148.93, 150.01, 151.81, 152.01, 153.32, 153.88, 155.38, 158.09, 159.21, 178.16, 178.84 ppm.

Preparation of $[Ru(bpy)_2(acac)]Cl_2$. $[Ru(bpy)_2(acac)]Cl_2$ was prepared according to previous report.[15] Yield: 72.4%. reddish brown powder. ^{1}H NMR (600 MHz, DMSO-d^6) δ 1.80 (s, 6H), 5.37 (s, 1H), 7.24-7.26 (t, 2H, *J* = 7.2 Hz), 7.70-7.71 (d, 2H, *J* = 5.4 Hz), 7.75-7.80 (m, 2H), 7.84-7.89 (m, 2H), 8.18-8.21 (t, 2H, *J* = 7.9 Hz), 8.66-8.67 (d, 2H, *J* = 5.3 Hz), 8.71-8.72 (d, 2H, *J* = 8.0 Hz), 8.84-8.85 (d, 2H, *J* = 8.0 Hz).

Stability Studies

The stability of complexes **1**, **2** and curcumin were recorded on a Shimadzu UV2600 UV-vis spectrophotometer equipped with a thermostatically controlled cell holder. The stock solution of the tested complexes were dissolved in MeOH, and then diluted to 20 μM with Hepes buffer (10 mM, pH 7.2). The UV-vis spectra were recorded every 10 min at 298 K.

log *P* Determination

Excess complexes **1**, **2** and $[Ru(bpy)_2(acac)]Cl_2$ were dissolved in n-octanol (presaturated with water) and then combined with an equal volume of deionized water (presaturated with octanol). The mixed solution was strongly shaken for 2 h and then centrifuged for 15 min to remove undissolved complexes and completely achieve phases separation. The concentrations of complexes in two phases were determined through standard working equation using UV-Vis spectroscopy. The log *P* values were measured using this formula:

$$\log P = \log (C_{octanol}/C_{water})$$

DFT Calculation

The structures of complexes **1** and **2** were optimized at the M06-L/6-31G*//LanL2DZ level in the gas phase at 310.15 K and 1 atm.[29] All calculations were carried out using the Gaussian 09 program package.[30]

Cell Culture

A549 (human non-small-cell lung cancer), MCF-7 (human breast adenocarcinoma cell line) and SGC7901 (human gastric cancer cell line) were incubated in culture medium containing 10% fetal bovine serum (FBS), 100 mg/mL of streptomycin and 100 mg/mL of penicillin in a sterile incubator of 5% CO_2 and 95% air at 37 °C.

In Vitro Cytotoxicity

The cytotoxicity of complexes **1**, **2**, cisplatin, $[Ru(bpy)_3]Cl_2$, and $[Ru(bpy)_2(acac)]Cl_2$ against three cancer cell lines was evaluated by means of MTT assay. Cells with excellent viability were dispersed into 96-well plates at a density of 10^4/well and then incubated for 24 h at 37 °C in a 5% CO_2 humidified air incubator. The test compounds were dissolved with DMF and then diluted with culture medium to the six required concentrations (1.56, 3.13, 6.25, 12.5, 25, 50 μM). The final concentration of DMF was less than 0.4%. Cisplatin was dissolved and diluted with culture medium to same concentrations. As for the negative control, 0.4% DMF was added. Then these diluted solutions were added to test wells, and incubated with cells at 37 °C for 72 h. After that, the cells were treated with MTT (5 mg/mL) for additional 5 h. Then the culture medium involving MTT was removed and 150 μL of DMSO was added. Finally, the activity of complexes were measured by an enzyme-labeling analyzer at UV absorption intensity of 570/630 nm. The final experimental data was analyzed by *SPSS* software through three parallel experiments.

Calcein AM and Propidium Iodide (PI) Co-Staining

For Calcein AM and propidium iodide (PI) co-staining assay, A549 cells (10^5 per well) were seeded and cultured in confocal dishes overnight at 37 °C. Then complexes **1** and **2** were added to the cells with the final concentration of 10 μM. After 24 h incubation, the cells were washed with PBS and stained with Calcein AM/PI Double Stain Kit according to the instruction manual. Fluorescence images of the stained cells were then taken using a confocal microscope. For PI channel, the excitation wavelength was 561 nm and the emission wavelength range was 600-640 nm. For calcein AM channel, the excitation wavelength was 488 nm and the emission was detected at 500-540 nm.

DNA Competitive Binding Experiment

The experiments were performed by combining stock solutions of **1** or **2** in MeOH to the mixed solution of 100 μM CT-DNA and 50 μM EtBr under physiological conditions (5 mM Tris-HCl/10 mM NaCl buffer solution, pH 7.2). The changes of the fluorescence emission spectra with an excitation at 537 nm were recorded after each successive addition of the tested complexes (0-14 μM) and incubation at room temperature for 5 min to complete the interaction.

Molecular Docking

Molecular docking studies were performed using an autodock 4.2 package. The crystal structure of the DNA duplex structure (PDB: 4jd8) were obtained from the protein data bank. The docking simulation process was conducted for 200 rounds with the lamarckian genetic algorithm search method. Each round of docking operations required 2500000 energy optimizations.

Dalton Transactions Accepted Manuscript

This journal is © The Royal Society of Chemistry 20xx

Please do not adjust margins

View Article Online
DOI: 10.1039/D0DT01040E

During the docking operation, the structure of DNA remained fixed, and binding energy optimizations were performed by rotation of the complexes. The final docking results of the complexes and DNA were output through PyMOL software.

Cell Uptake

A549 and MCF-7 cells with good viability were transferred into 6-well plates at 37 °C. After 12 h cultivation in medium, cells were co-incubated with complexes **1**, **2** and $[Ru(bpy)_2(acac)]Cl_2$ (5 μM) for 12 h. After the supernatants were removed, cells were collected and washed 3 times with ice-cold PBS, then centrifuged for 10 minutes, and resuspended in PBS (1 mL). The nuclei component for measurement were extracted using commercial nuclear extraction kit (Solarbio). The remaining samples were then digested with HNO_3 (65%, 200 μL) for 24 h at room temperature. After three parallel experiments, the Ru content were measured by ICP-MS.

Western Blot Assay

A549 cells were transferred to a 6-well plate and incubated overnight at 37 °C. Complexes **1** and **2** were diluted to the required concentrations (0.1, 0.5, 2.5, 10 μM, the final concentration of DMF was less than 0.4%) with culture medium, and added to the cells for 24 h incubation at 37 °C. For the negative control, 0.4% DMF was added. Afterwards, the proteins extracted from the lysate were detached by 8-12% SDA-PAGE (sodium dodecyl sulfate-polyacrylamide gel electrophoresis) and transferred to the PVDF (polyvinylidene difluoride) membrane. Then the protein membrane was rinsed for 1-2 minutes, and the blocking solution TBST (Tris buffered saline plus 0.1% Tween 20) was added. After that, this membrane was incubated with the preliminary antibody (MEK1) overnight at 4 °C. A suitable dilution of horseradish peroxidase (HRP)-labeled secondary antibody was further added and incubated for 1 h at room temperature. Western blotting can be detected using Ingen's Enlight and other sensitive ECL luminescent solutions. High-sensitivity ECL luminescent solution was used to detect proteins. The loading control used Glyceraldehyde 3-phosphate dehydrogenase (GAPDH).

Cell Cycle Distribution

A549 cells were seeded at the density of 2×10^5 per well in a 6-well plate and incubated for 24 h in a 37 °C incubator. The complexes were dissolved with DMF and diluted with medium to concentrations of 1 μM and 5 μM. The final concentration of DMF was less than 0.4%. As for the negative control, 0.4% DMF was added. After 24 h incubation, the cells were washed with PBS and fixed with 70% ethanol for 24 h at 4 °C. After centrifugation to remove ethanol from the sample, the cells were stained by adding PI (50 μg/mL) and RNase Staining Buffer (100 μg/mL) and incubated for 20 min. Flow cytometry (FAC Scan, Becton Dickenson) was used to detect the number of cells in each phase.

Apoptosis studies by Flow Cytometry

A549 cells with good viability were transferred to a 6-well plate and cultured overnight at 37 °C. Complexes **1** and **2** were dissolved with DMF and diluted to 1 μM and 5 μM by culture medium. The final concentration of DMF was less than 0.4%. For the negative control, 0.4% DMF was added. The diluted complexes were added to these wells, and incubated for 24 h. The cells were then collected with trypsin and washed with cold PBS. Then, cells were centrifugated (5 min, 2000 rpm), then washed twice with cold water and resuspended in binding buffer (10 mM Heps, 140 mM NaCl, 2.5 mM $CaCl_2$, pH 7.4). Afterwards, cells were stained with 3 μL of Annexin V-FITC (100 ng/mL) and 3 μL of PI (2 μg/mL). Cellular fluorescence was quantified by flow cytometry (FAC Scan, Becton Dickenson) using the Annexin V-FITC Apoptosis Detection Kit (Roche) and analyzed by *Cell Quest* software.

Hoechst 33358 Staining for Apoptosis Studies

A549 cells were seeded in a 6-well plate and incubated overnight in a 37 °C incubator. Then the cells were co-cultured with complexes **1**-**2** (2.5 μM) for 24 h. Afterwards, cells were washed three times with PBS buffer solution, and stained with Hoechst 33358 for 10 min at 37 °C. After removing the staining solution, the apoptosis cells were detected using fluorescence microscopy with excitation wavelength of 346 nm.

Conclusions

In summary, two curcumin-based Ru(II)-polypyridyl complexes were prepared and characterized. In vitro tests indicated that the resulting Ru(II)-polypyridyl complexes showed much superior activity to those of reference compounds curcumin, cisplatin, $[Ru(bpy)_3]Cl_2$ and $[Ru(bpy)_2(acac)]Cl_2$ against the tested cancer cell lines, especially complex **2**, which were 17.0-, 5.7- and 4.8-fold as potent as $[Ru(bpy)_3]Cl_2$, curcumin and cisplatin, respectively, demonstrating that the Ru(II)-polypyridyl moieties and curcumin have a positive cooperative effect on cancer cells. DNA binding study revealed that complex **1** may interact with DNA through groove binding, while complex **2** is proposed to interact with DNA via intercalation. Further results of western blot assay showed that the resulting Ru(II) complexes have the potential to prevent the phosphorylation of MEK1 and ERK1 in A549 cancer cells. Hence, we proposed that the resulting Ru(II)-polypyridyl-curcuminato complexes induces apoptosis in cancer cells through DNA intercalation and by inhibiting the MEK/ERK signaling pathway, which is the first example of a Ru(II)-polypyridyl complex to affect ERK signaling pathway as well as DNA interaction. However, considering the complexities of the cellular system, there may be existence of other targets for the greatly enhanced cytotoxicity of **1** and **2**. Thus, exploring Ru(II)-polypyridyl complexes with multiple targets and different modes of action is an effective approach for antitumor drug development.

Conflicts of interest

There are no conflicts to declare.

Published on 18 June 2020. Downloaded by East Carolina University on 6/18/2020 11:39:13 AM.

Dalton Transactions Accepted Manuscript

Please do not adjust margins

View Article Online
DOI: 10.1039/D0DT01040E

Published on 18 June 2020. Downloaded by East Carolina University on 6/18/2020 11:39:13 AM.

Dalton Transactions Accepted Manuscript

Acknowledgements

We are grateful to the National Natural Science Foundation of China (Grant 21601034)，Jiangsu Province Natural Science Foundation (Grant BK20160664) and Fundamental Research Funds for the Central Universities (2242020K40031) for financial aid to this work.

References

1 (a) N. J. Wheate, S. Walker, G. E. Craig and R. Oun, *Dalton Trans.*, 2010, **39**, 8113-8127. (b) N. P. E. Barry and P. J. Sadler, *Chem. Commun.*, 2013, **49**, 5106-5131. (c) T. C. Johnstone, K. Suntharalingam and S. J. Lippard, *Chem. Rev*., 2016, **116**, 3436-3486. (d) X. Wang and Z. Guo. *Chem. Soc. Rev*., 2013, **42**, 202-224. (e) Y. Sun, J. Zhao and Z. Ji, *Chem. Biodivers*., 2017, **14**, e1700348. (f) J. Zhao, S. Gou, Y. Sun, L. Fang and Z. Wang, *Inorg. Chem*., 2012, **51**, 10317-10324.

2 (a) G. Gasser, I. Ott and N. Metzler-Nolte, *J. Med. Chem.*, 2011, **54**, 3-25. (b) C. G. Hartinger and P. J. Dyson, *Chem. Soc. Rev.*, 2009, **38**, 391-401. (c) Y. Sun, H. Wei, Q. Zhang and X. Zhao, *Chem. Biodivers*., 2019, **16**, e1800373. (d) J. Zhao, S. Gou, F. Liu, Y. Sun, and C. Gao. *Inorg. Chem*., 2013, **52**, 8163-8170.

3 (a) R. Trondl, P. Heffeter, C. R. Kowol, M. A. Jakupec, W. Berger and B. K. Keppler, *Chem. Sci.* 2014, **5**, 2925-2932. (b) C. G. Hartinger, S. Zorbas-Seifried, M. A. Jakupec, B. Kynast, H. Zorbas and B. K. Keppler, *J. Inorg. Biochem*., 2006, **100**, 891-904. (c) S. Monro, K. L. Colón, H. Yin, J. Roque III, P. Konda, S. Gujar, R. P. Thummel, L. Lilge, C. G. Cameron and S. A. McFarland, *Chem. Rev*., 2019, **119**, 797-828. (d) J. Zhao, W. Li, S. Gou, S. Li, S. Lin, Q. Wei and G. Xu, *Inorg. Chem*., 2018, **57**, 8396-8403.(e) J. Zhao, N. Liu, S. Sun, S. Gou, X. Wang, Z. Wang, X. Li, W. Zhang, *J. Inorg. Biochem.*, 2019, **196**, 110684-110692. (f) J. Zhao, D. Zhang, W. Hua, W. Li, G. Xu and S. Gou, *Organometallics*., 2018, **37**, 441-447.

4 (a) F. E. Poynton, S. A. Bright, S. Blasco, D. C. Williams, J. M. Kelly and T. Gunnlaugsson, *Chem. Soc. Rev.*, 2017,**46**, 7706-7756. (b) L. Zeng, P. Gupta, Y. Chen, E. Wang, L. Ji, H. Chao and Z. Chen., *Chem. Soc. Rev.*, 2017,**46**, 5771-5804.

5 (a) A. Notaro and G. Gasser, *Chem. Soc. Rev.*, 2017, **46**, 7317-7337. (b) M. R. Gill and J. A. Thomas, *Chem. Soc. Rev.*, 2012, **41**, 3179-3192. (c) F. Jia, S. Wang, Y. Man, P. Kumar and B. Liu, *Molecules.*, 2019, **24**, 769-786.

6 (a) S. P. Foxon, M. A. H. Alamiry, M. G. Walker, A. J. H. M. Meijer, I. V. Sazanovich, J. A. Weinstein, J. A. Thomas, *J. Phys. Chem. A*., 2009, **113**, 12754-12762. (b) M. G. Walker, V. Ramu, A. J. H. M. Meijer, A. Das and J. A. Thomas, *Dalton Trans*., 2017, **46**, 6079-6086. (c) G.-B. Jiang, Y.-Yin Xie, G.-J. Lin, H.-L. Huang, Z.-H. Liang and Y.-J. Liu, *J. Photochem. Photobiol. B: Biol*., 2013, **129**, 48-56. (d) Z.-P. Zeng, Q. Wu, F.-Y. Sun, K.-D. Zheng, and W.-J. Mei, *Inorg. Chem*., 2016, **55**, 5710−5718. (e) N. Tian, Y. Feng, W. Sun, J. Lu, S. Lu, Y. Yao, C. Li, X. Wang and Q. Zhou, *Dalton Trans*., 2019, **48**, 6492–650.

7 (a) T. Esatbeyoglu, P. Huebbe, I. M. A. Ernst, D. Chin, A. E. Wagner and G. Rimbach, *Angew. Chem. Int. Ed*., 2012, **51**, 5308-5332. (b) P. Anand, A. B. Kunnumakkara, R. A. Newman and B. B. Aggarwal, *Mol. Pharmaceutics.* 2007, **4**, 807-818. (c) K. M. Nelson, J. L. Dahlin, J. Bisson, J. Graham, G. F. Pauli and M. A. Walters, *J. Med. Chem*., 2017, **60**, 1620-1637. (d) P. B. Luis, W. E. Boeglin, and C. Schneider, *Chem. Res. Toxicol*., 2018, **31**, 269-276.

8 (a) Y. Li, Q. Zou, C. Yuan, S. Li, R. Xing and X. Yan, *Angew. Chem. Int. Ed*., 2018, **57**, 17084-17088. (b) O. Naksuriya, S. Okonogi, R. M. Schiffelers and W. E. Hennink, *Biomaterials.*, 2014, **35**, 3365-3383. (c) F. Zhu, G. Tan, Y. Jiang, Z. Yu and F. Ren, *Biomater. Sci*., 2018, **6**, 2905-2917.

9 (a) S. Wanninger, V. Lorenz, A. Subhan and F. T. Edelmann, *Chem. Soc. Rev.*, 2015, **44**, 4986-5002. (b) S. Banerjee and A. R. Chakravarty, *Acc. Chem. Res*., 2015, **48**, 2075-2083. (c) M. Pröhl, U. S. Schubert, W. Weigand and M. Gottschaldt, *Coordin. Chem. Rev*., 2016, **307**, 32-41. (d) S. Huang, Y. Liang, C. Huang, W. Su, X. Lei, Y. Liu and Q. Xiao, *Lumin.*, 2016, **31**, 1384–1394.

10 (a) A. Valentini, F. Conforti, A. Crispini, A. De Martino, R. Condello, C. Stellitano, G. Rotilio, M. Ghedini, G. Federici, S. Bernardini and D. Pucci, *J. Med. Chem*., 2009, **52**, 484–491. (b) D. Pucci, A. Crispini, B. S. Mendiguchía, S. Pirillo, M. Ghedini, S. Morelli and L. D. Bartolo, *Dalton Trans.*, 2013, **42**, 9679-9687. (c) A, Bhattacharyya, A. Dixit, K. Mitra, S. Banerjee, A. A. Karande and A. R. Chakravarty, *Med. Chem. Commun*., 2015, **6**, 846−851. (d) A. K. Renfrew, N. S. Bryce and T. W. Hambley, *Chem. Sci*., 2013, **4**, 3731-3739. (e) A. Colombo, M. Fontani, C. Dragonetti, D. Roberto, J. A. G. Williams, R. S. di Perrotolo, F. Casagrande, S. Barozzi and S. Polo, *Chem. Eur. J*., 2019, **25**,7948–7952. (f) M. C. Henriques, M. A. F. Faustino, A. M. S. Silva, J. Felgueiras, M. Fardilhab and S. S. Brag, *J. Coord. Chem*., 2017, **70**, 2393-2408.

11 F. Caruso, M. Rossi, A. Benson, C. Opazo, D. Freedman, E. Monti, M.B. Gariboldi, J. Shaulky, F. Marchetti, R. Pettinari and C. Pettinari, *J. Med. Chem*., 2012, **55**, 1072–1081.

12 F. Caruso, R. Pettinari, M. Rossi, E. Monti, M. B. Gariboldi, F. Marchetti, C. Pettinari, A. Caruso, M. V. Ramani and G. V. Subbaraju. *J. Inorg. Biochem.*, 2016, **162**, 44–51.

13 (a) R. Pettinari, F. Marchetti, F. Condello, C. Pettinari, G. Lupidi, R. Scopelliti, S. Mukhopadhyay, T. Riedel and P. J. Dyson, *Organometallics*., 2014, **33**, 3709-3715. (b) R. Pettinari, F. Condello, F. Marchetti, C. Pettinari, P. Smoleński, T. Riedel, R. Scopelliti, and P. J. Dyson, *Eur. J. Inorg. Chem.*, 2017, 2905–2910.

14 (a) A.-C. Munteanu, A. Notaro, M. Jakubaszek, J. Cowell, M. Tharaud, B. Goud, V. Uivarosi and G. Gasser, *Inorg. Chem*., 2020, **59**, 4424−4434. (b) I. Gurgul, O. Mazuryk, M. Łomzik, P. C. Gros, D. R.-Zbik and M. Brindell, *Metallomics.*, DOI: 10.1039/d0mt00019a. (c) S.-Q. Zhang, T.-T. Meng, J. Li, F. Hong, J. Liu, Y. Wang, L.-H. Gao, H. Zhao and K.-Z. Wang, *Inorg. Chem*., 2019, **58**, 14244−14259. (d) B. Peña, S. Saha, R. Barhoumi, R. C. Burghardt and K. R. Dunbar, *Inorg. Chem*., 2018, **57**, 12777-12786. (e) C. Griffith, A. S. Dayoub, T. Jaranatne, N. Alatrash, A. Mohamedi, K. Abayan, Z. S. Breitbach, D. W. Armstrong and F. M. MacDonnell, *Chem. Sci*., 2017, **8**, 3726-3740.

15 P. Srivastava, M. Shukla, G. Kaul, S. Chopra and A. K. Patra, *Dalton Trans*., 2019, **48**, 11822–11828.

16 (a) R. M. Hartshorn and J. K. Barton, *J. Am. Chem. Soc.*, 1992, **114**, 5919-5925. (b) A. W. McKinley, P. Lincoln and E. M. Tuite, *Coord. Chem. Rev*., 2011, **255**, 2676−2692.

17 (a) Y. Sun, L. E. Joyce, N. M. Dickson and C. Turro, *Chem. Comm*., 2010, **46**, 6759-6761. (b) X. Chen, F. Gao, W. Y. Yang, Z. X. Zhou, J. Q. Lin, and L. N. Ji, *Chem. Biodivers.*, 2013, **10**, 367-384.

18 (a) C. Gossens, A. Dorcier, P. J. Dyson, and U. Rothlisberger, *Organometallics*., 2007, **26**, 3969-3975. (b) Z. Liu, A. Habtemariam, A. M. Pizarro, S. A. Fletcher, A. Kisova, O. Vrana, L. Salassa, P. C. A. Bruijnincx, G. J. Clarkson, V. Brabec and P. J. Sadler, *J. Med. Chem*., 2011, **54**, 3011–3026. (c) H. Ahmad, A. Wragg, W. Cullen, C. Wombwell, A. J. H. M. Meijer, and J. A. Thomas, *Chem. Eur. J*., 2014, **20**, 3089-3096.

19 J. Zhao, S. Li, X. Wang, G. Xu and S. Gou, *Inorg. Chem*., 2019, **58**, 2208-2217.

20 Z. Luo, L. Yu, F. Yang, Z. Zhao, B. Yu, H. Lai, K.-H. Wong, S.-M. Ngai, W. Zheng and T. Chen, *Metallomics*., 2014, **6**, 1480-1490.

21 S. Mardanya, S. Karmakar, D. Mondal and S. Baitalik, *Inorg. Chem.*, 2016, **55**, 3475-3489.

 This journal is © The Royal Society of Chemistry 20xx

View Article Online
DOI: 10.1039/D0DT01040E

Published on 18 June 2020. Downloaded by East Carolina University on 6/18/2020 11:39:13 AM.

22 S. Ramakrishnan, D. Shakthipriya, E. Suresh, V. S. Periasamy, M. A. Akbarsha and M. Palaniandavar, *Inorg. Chem*., 2011, **50**, 6458–6471.
23 (a) J. P. Hall, D. Cook, S. R. Morte, P. McIntyre, K. Buchner, H. Beer, D. J. Cardin, J. A. Brazier, G. Winter, J. M. Kelly and C. J. Cardin, *J. Am. Chem. Soc*., 2013, **135**, 12652-12659. (b) G. M. Morris, R. Huey, W. Lindstrom, M. F. Sanner, R. K. Belew, D. S. Goodsell and A. J. Olson, *J. Comput. Chem*., 2009, **30**, 2785-2791.
24 K.-K. Liao, M.-J. Wu, P.-Y. Chen, S.-W. Huang, S.-J. Chiu, C.-T. Ho and J.-H. Yen, *J. Agric. Food Chem*., 2012, **60**, 433−443.
25 (a) J. Chen, R. Bian, J. Li, L. Qiu, B. Lu and X. Ouyang, *Ecotox Environ Safe*., 2019, **173**, 142-148. (b) M. Mahnashi, S. M. Elgazwi, M. S. Ahmed, F. T. Halaweish, *Eur. J. Med. Chem*., 2019, **173**, 294-304. (c) M. E. Van Dort, H. Hong, H. Wang, C. A. Nino, R. L. Lombardi, A. E. Blanks, S. Galbán, and B. D. Ross, *J. Med. Chem*., 2016, **59**, 2512-2522. (d) M. E. Van Dort, S. Galbán, C. A. Nino, H. Hong, A. A. Apfelbaum, G. D. Luker, G. M. Thurber, L. Atangcho, C. G. Besirli and B. D. Ross, *ACS Med. Chem. Lett*., 2017, **8**, 808-813. (e) A. M. Kidger, J. Sipthorp and S. J. Cook, *Pharmacol Therapeut.*, 2018, **187**, 45-60. (f) F. Zou, Y. Yang, T. Ma, J. Xi, J. Zhou, X. Zha, *Med Chem Res*., 2017, **26**, 701-713.
26 (a) J. Sun, Y. Niu, C. Wang, H. Zhang, B. Xie, F. Xu, H. Jin, Y. Peng, L. Liang and P. Xu, *Bioorgan Med Chem.*, 2016, **24**, 3472-3482. (b) Q. Dong, B. Yang, J. Han, M. Zhang, W. Liu, X. Zhang, H. Yu, Z. Liu, S. Zhang, T. Li, D. Wu, X. Ji and S. Duan, *Cancer Lett*., 2019, **455**, 60−72.
27 (a) S. Jin, Y. Guo, D. Song, Z. Zhu, Z. Zhang, Y. Sun, T. Yang, Z. Guo and X. Wang, *Inorg. Chem*., 2019, **58**, 6507-6516. (b) S. Zhang, H. Yuan, Y. Guo, K. Wang, X. Wang and Z. Guo. *Chem. Commun*., 2018, **54**, 11717-11720.
28 (a) L. Wang, H. Yin, M. A. Jabed, M. Hetu, C. Wang, S. Monro, X. Zhu, S. Kilina, S. A. McFarland and W. Sun, *Inorg. Chem*., 2017, **56**, 3245-3259. (b) D. Phapale, R. Ghosh and D. Das, *Inorg. Chem*., 2017, **56**, 6310-6317.
29 (a) Y. Zhao and D. G. Truhlar, *Theor. Chem. Acc*., 2008, **120**, 215−241. (b) W. R. Wadt and P. J. Hay, *J. Chem. Phys*., 1985, **82**, 284−298.
30 M. J. Frisch, G. W. Trucks, H. B. Schlegel, G. E. Scuseria, M. A. Robb, J. R. Cheeseman, G. Scalmani, V. Barone, B. Mennucci, G. A. Petersson, H. Nakatsuji, M. Caricato, X. Li, H. P. Hratchian, A. F. Izmaylov, J. Bloino, G. Zheng, J. L. Sonnenberg, M. Hada, M. Ehara, K. Toyota, R. Fukuda, J. Hasegawa, M. Ishida, T. Nakajima, Y. Honda, O. Kitao, H. Nakai, T. Vreven, J. A. Jr. Montgomery, J. E. Peralta, F. Ogliaro, M. J. Bearpark, J. Heyd, E. N. Brothers, K. N. Kudin, V. N. Staroverov, R. Kobayashi, J. Normand, K. Raghavachari, A. P. Rendell, J. C. Burant, S. S. Iyengar, J. Tomasi, M. Cossi, N. Rega, N. J. Millam, M. Klene, J. E. Knox, J. B. Cross, V. Bakken, C. Adamo, J. Jaramillo, R. Gomperts, R. E. Stratmann, O. Yazyev, A. J. Austin, R. Cammi, C. Pomelli, J. W. Ochterski, R. L. Martin, K. Morokuma, V. G. Zakrzewski, G. A. Voth, P. Salvador, J. J. Dannenberg, S. Dapprich, A. D. Daniels, O. Farkas, J. B. Foresman, J. V. Ortiz, J. Cioslowski and D. J. Fox, Gaussian 09, version E01; Gaussian, Inc.: Wallingford, CT, 2009.

Dalton Transactions Accepted Manuscript

View Article Online
DOI: 10.1039/D0DT01040E

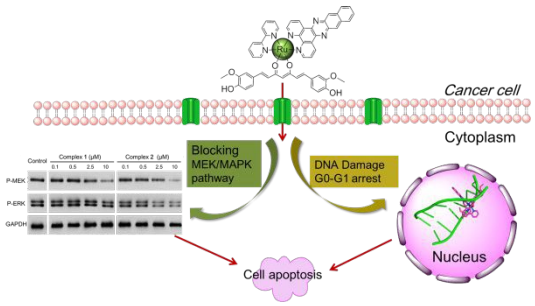

Ru(II)-polypyridyl-curcuminato complex induces cancer cells apoptosis through DNA intercalation and MEK/ERK signaling pathway.

Published on 18 June 2020. Downloaded by East Carolina University on 6/18/2020 11:39:13 AM.

Dalton Transactions Accepted Manuscript